Materials Physics and Mechanics 37 (2018) 25-33 Received: December 22, 2017

FINITE ELEMENT HOMOGENIZATION MODELS OF BULK MIXED PIEZOCOMPOSITES WITH GRANULAR ELASTIC INCLUSIONS IN ACELAN PACKAGE

A.B. Kudimova[1], D.K. Nadolin[1], A.V. Nasedkin[1], P.A. Oganesyan[1], A.N. Soloviev[1,2]*

[1]I.I. Vorovich Institute of Mathematics, Mechanics and Computer Science, Southern Federal University, Miltchakova Str., 8a, Rostov-on-Don, 344090, Russia

[2]Department of Theoretical and Applied Mechanics, Don State Technical University, Gagarin Sq., 1, Rostov-on-Don, 344000, Russia

*e-mail: solovievarc@gmail.com

Abstract. The paper presents the methods for solving the homogenization problems for two-phase piezoelectric composites, which are implemented in ACELAN-COMPOS finite element package, developed by the authors. The considered composites consist of piezoelectric skeleton and elastic inclusions. The effective moduli method is used to determine the effective properties of the composite. In this method, the static electroelasticity problems with special boundary conditions are set for a representative volume of the composite. These problems are solved numerically using the finite element method. The developed algorithm for generating representative volumes for the composites with granular inclusions is described in details. The work of the algorithm is illustrated by an example of a composite made of PZT-4 piezoceramic with inclusions of α-corundum.

Keywords: piezoelectricity; two-phase piezocomposite; effective moduli; representative volume; finite element method; finite element software.

1. Introduction

Piezoelectric materials are widely used in modern engineering due to their ability to convert electrical energy into mechanical energy and *vice versa*, which is known as the piezoelectric effect. In order to improve the efficiency of these materials, the piezoelectric composites, based on piezoceramic skeleton, have been developed recently. Porous piezoceramic materials appeared perspective for use as the elements for acoustic transmitters and as renewable energy sources. As it turned out, in comparison with dense ceramics, porous piezoceramics had small acoustic impedance, but sufficiently high values of piezoelectric sensitivities and thickness piezomoduli. However, porous piezoceramics are less strong compared with dense ceramics. To improve the mechanical properties of porous piezoceramics, more rigid crystallites can be added into ceramic composites [1, 2].

The subject of this research is the piezocomposites of piezoceramics – crystallite (elastic inclusions) type. We use the effective moduli method and finite element technique implemented in our new own-developed software ACELAN-COMPOS [3]. In order to find the effective moduli of inhomogeneous body, we set special static piezoelectric problems for a representative volume. These problems differ by the boundary conditions, which are imposed on the representative volume surfaces. Special formulae are derived to calculate the effective moduli of piezoelectric media with arbitrary anisotropy. Based on these formulae,

http://dx.doi.org/10.18720/MPM.3712018_4

we can find the full set of effective moduli for ceramic polycrystalline piezocomposites using finite element method.

As a representative volume, we consider a cube evenly divided into cubic eight-node finite elements. For a mixed two-phase composite, such element can have piezoelectric properties for material of the skeleton or elastic properties for the material of inclusions. Inclusions are simulated as granules, consisting of one or more structural elements not connected with other granules (composite of 3-0 connectivity type [4]). The input user parameters are the minimum and maximum granule size, as well as the maximum quantum of inclusions in the representative volume. Random choice of the supporting element for the granule ensures the stochastic resulting distribution. The granule grows according to an algorithm that allows the granule to be shaped as close to the ball as possible, while avoiding unnaturally elongated elements.

To provide an example, we consider a polycrystalline piezoceramic with sapphire (α-corundum) crystallites Al_2O_3 as inclusions. The effective moduli of the inclusions are calculated as the average moduli of monophase polycrystallite of trigonal system. The results of calculations give the full set of the effective moduli.

2. Homogenization of two-phase piezoelectric composite by effective moduli method

Let Ω be a representative volume of a two-phase composite heterogeneous body composed of two piezoelectric materials $\Omega = \Omega^{(1)} \cup \Omega^{(2)}$, where the phase $\Omega^{(1)}$ is the skeleton or the main medium and the phase $\Omega^{(2)}$ is the inclusion; $\Gamma = \partial\Omega$ is the external boundary of the volume Ω; $\mathbf{x} = \{x_1, x_2, x_3\}$ is the vector of the spatial coordinates.

In order to determine the effective moduli of the composite, let us consider the following static piezoelectric boundary problem

$$\mathbf{L}^*(\nabla)\cdot\mathbf{T} = 0,\ \nabla\cdot\mathbf{D} = 0,\ \mathbf{T} = \mathbf{c}\cdot\mathbf{S} - \mathbf{e}^*\cdot\mathbf{E},\ \mathbf{D} = \mathbf{e}\cdot\mathbf{S} + \boldsymbol{\kappa}\cdot\mathbf{E}, \tag{1}$$

$$\mathbf{S} = \mathbf{L}(\nabla)\cdot\mathbf{u},\ \mathbf{E} = -\nabla\varphi,\ \mathbf{L}^*(\nabla) = \begin{bmatrix} \partial_1 & 0 & 0 & 0 & \partial_3 & \partial_2 \\ 0 & \partial_2 & 0 & \partial_3 & 0 & \partial_1 \\ 0 & 0 & \partial_3 & \partial_2 & \partial_1 & 0 \end{bmatrix},\ \nabla = \begin{Bmatrix} \partial_1 \\ \partial_2 \\ \partial_3 \end{Bmatrix}, \tag{2}$$

$$\mathbf{u} = \mathbf{L}^*(\mathbf{x})\cdot\mathbf{S}_0,\ \varphi = -\mathbf{x}\cdot\mathbf{E}_0,\ \mathbf{x}\in\Gamma, \tag{3}$$

where $\mathbf{T} = \{\sigma_{11}, \sigma_{22}, \sigma_{33}, \sigma_{23}, \sigma_{13}, \sigma_{12}\}$ is the array of the stress components σ_{ij}; $\mathbf{S} = \{\varepsilon_{11}, \varepsilon_{22}, \varepsilon_{33}, 2\varepsilon_{23}, 2\varepsilon_{13}, 2\varepsilon_{12}\}$ is the array of the strain components ε_{ij}; $\mathbf{D}$ is the electric flux density vector or the electric displacement vector; $\mathbf{E}$ is the electric field vector; $\mathbf{u}$ is the vector-function of mechanical displacement; φ is the function of electric potential; $\mathbf{c} = \mathbf{c}^E$ is the 6×6 matrix of elastic stiffness moduli; $\mathbf{e}$ is the 3×6 matrix of piezoelectric moduli; $\boldsymbol{\kappa} = \boldsymbol{\varepsilon}^S$ is the 3×3 matrix of dielectric permittivity moduli; $\mathbf{c} = \mathbf{c}^{(i)}$, $\mathbf{e} = \mathbf{e}^{(i)}$, $\boldsymbol{\kappa} = \boldsymbol{\kappa}^{(i)}$ for $\mathbf{x}\in\Omega^{(i)}$; $\mathbf{S}_0 = \{\varepsilon_{011}, \varepsilon_{022}, \varepsilon_{033}, 2\varepsilon_{023}, 2\varepsilon_{013}, 2\varepsilon_{012}\}$; ε_{0km} are some constant values that do not depend on $\mathbf{x}$; $\mathbf{E}_0$ is some constant vector; $(...)^*$ is the transpose operation; and $(...)\cdot(...)$ is the scalar product operation.

By using (3), we can select such boundary conditions that enable us to obtain obvious expressions for the effective moduli:

$$\text{I.}\ \ \mathbf{S}_0 = S_0\mathbf{h}_\beta, \mathbf{E}_0 = 0\ \Rightarrow c^{\text{eff}}_{\alpha\beta} = <T_\alpha>/S_0,\ e^{\text{eff}}_{i\beta} = <D_i>/S_0, \tag{4}$$

$$\text{II.}\ \ \mathbf{S}_0 = 0,\ \mathbf{E}_0 = E_0\mathbf{e}_m,\ \Rightarrow e^{\text{eff}}_{m\alpha} = -<T_\alpha>/E_0,\ \kappa^{\text{eff}}_{im} = <D_i>/E_0, \tag{5}$$

where $S_0 = \text{const}$; $E_0 = \text{const}$; β is a fixed index ranging from 1 to 6; m is a fixed index ranging from 1 to 3; $\mathbf{h}_\beta$ is the vector from six-dimensional basic set for the components of the strain tensor; $\mathbf{h}_j = \mathbf{e}_j\mathbf{e}_j$, $j = 1, 2, 3$; $\mathbf{h}_4 = (\mathbf{e}_2\mathbf{e}_3 + \mathbf{e}_3\mathbf{e}_2)/2$; $\mathbf{h}_5 = (\mathbf{e}_1\mathbf{e}_3 + \mathbf{e}_3\mathbf{e}_1)/2$; $\mathbf{h}_6 = (\mathbf{e}_1\mathbf{e}_2 + \mathbf{e}_2\mathbf{e}_1)/2$; $\mathbf{e}_j$ are the orts of the Cartesian coordinate system; $\alpha = 1, 2, ..., 6$; $i = 1, 2, 3$; hereinafter the angle brackets denote the averaged by the volume Ω values: $< (...) >= (1/|\Omega|)\int_\Omega (...)d\Omega$.

By using Equations (4), (5), from the solutions of six problems (1) – (4) for $\beta = 1, 2, ..., 6$, and from the finite element solutions of three problems (1) – (3), (5) for $m = 1, 2, 3$, we can obtain the full set of the effective moduli $c^{\text{eff}}_{\alpha\beta}$, $e^{\text{eff}}_{m\alpha}$, κ^{eff}_{im} for a two-phase piezoelectric composite. Note, that this technique is suitable when the phase $\Omega^{(2)}$ is presented by the elastic inclusions with $\mathbf{e}^{(2)} = 0$. The background and more detailed description of the considered approaches are presented in [3, 5].

3. The description of the algorithm for creating the 3-0 connectivity composite

In ACELAN-COMPOS, we simulate mixed composite materials using cubic eight-node or twenty-node elements in the representative volume. There are a number of algorithms in ACELAN-COMPOS for creating the representative volumes with different types of connectivity and with controlled characteristics of the internal structure [3]. A granule generation algorithm (3-0 connectivity algorithm) to model a composite with separate inclusions is used below. This section gives a detailed description of this algorithm.

Consider a granule as simply connected region of a specific material, consisting of one or more structural elements. The generation of granules occurs within a special area, called a domain. The domain is a cube, evenly divided along each side into eight smaller cubes. Thus, the domain consists of $8 \times 8 \times 8 = 512$ identical cubic elements. These elements are identified with the corresponding finite elements in the subsequent numerical calculations. The granule size, as well as its location within the domain, is determined randomly. The algorithm can build one or more granules in the domain. At the same time, it is guaranteed that the granules inside the domain will not be connected to each other.

As input data, the user specifies the percentage of granules material in the volume of the domain, as well as the minimum and maximum granule sizes. The process of the granule generation occurs sequentially until the user-defined percentage of their content is reached. When the percentage of granules is exceeded by adding any granule of minimum size the algorithm also terminates. During the execution of the algorithm, two obligatory conditions must be satisfied: the granules do not adhere to each other, and the skeleton of the basic material remains simply connected.

The supporting element for generating the granule is selected randomly inside the domain. The granule is grown by random selection of the candidate (for example, element number 1 in Fig. 1b) in one of six possible directions (Fig. 1a), the remaining directions fall into the queue with increasing numbering (Fig. 1b, light gray elements 2 – 4). Then the elements that border the selected element along the planes in terms of the degree of proximity to the granule center (Fig. 1b, elements 5 – 7) are added to this queue. This process is repeated according to the scheme presented in Fig. 2a (Fig. 1 and Fig. 2 show a two-dimensional area for the clarity of presentation). The generation of the granule is terminated when either the granule reaches the maximum size, or the queue of candidates for addition is exhausted. Upon completion of the construction, the granules of the elements, bordering the constructed granule, are excluded from the further distribution process (Fig. 2b, elements marked with a cross). This allows us to avoid the case of the granules merging

within the domain. At the same time, the merging of the granules, located on the domain border and belonging to different domains, is still possible.

(a) (b)

Fig. 1. (a) Supporting element of the granule and the possible directions, (b) order of adding elements to the granule.

(a) (b)

Fig. 2. (a) Order of adding the elements to the granule on the third step of the algorithm, (b) constructed granule with the elements, excluded from the subsequent construction.

When the granule construction is completed (Fig. 3), we check whether the addition of the granule of the minimum size will exceed the user-defined ratio. In case, the addition of the granule is possible, the process is repeated.

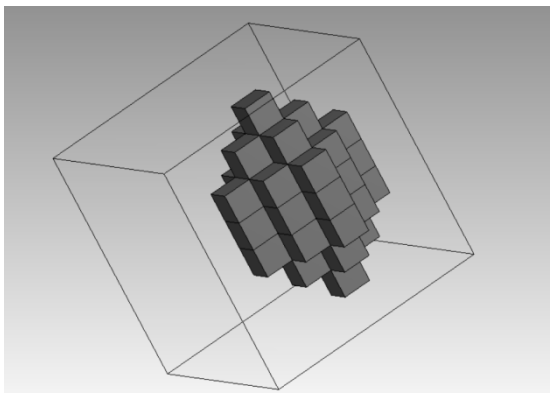

Fig. 3. Example of built granule.

If the queue of potential candidates for the granule extension is exhausted before the granule reaches a minimum size, then the granule does not form, and all the belonging elements are excluded from further consideration. The situation described can be explained as

follows: the subregion of the skeleton material, from which the supporting element is selected, is not large enough to accommodate a granule of the minimum volume.

The algorithm permits to generate the granules that do not exceed the maximum size of the granule. However, the cases when the granule is located near to the domain edges can lead to the creation of granules that exceed the maximum size.

4. The results of numerical experiments

As an example, in this section we will consider PZT/α-Al_2O_3 piezoceramic/monocrystal composite material. We determine the effective moduli of polycrystalline piezoceramic in two stages. At the first stage, we calculate the effective moduli for material of inclusions. At the second stage, we consider a piezocomposite with isotropic inclusions as a two-phase composite. Here we can use the models of representative volumes with elastic isotropic inclusions, described in the previous sections.

In accordance with [6], at the first stage we obtain the averaged moduli of α-corundum as an isotropic phase: $E^{(2)} = 40.26 \cdot 10^{10}$ N/m^2; $\nu^{(2)} = 0.23$; $c_{11}^{(2)} = 46.88 \cdot 10^{10}$ N/m^2, $c_{12}^{(2)} = 14.22 \cdot 10^{10}$ N/m^2; $\kappa^{(2)} = 10\varepsilon_0$. For dense piezoceramic PZT-4 we take the following material constants: $c_{11}^{(1)} = 13.9 \cdot 10^{10}$ N/m^2; $c_{12}^{(1)} = 7.78 \cdot 10^{10}$ N/m^2; $c_{13}^{(1)} = 7.43 \cdot 10^{10}$ N/m^2; $c_{33}^{(1)} = 11.5 \cdot 10^{10}$ N/m^2; $c_{44}^{(1)} = 2.56 \cdot 10^{10}$ N/m^2; $e_{31}^{(1)} = -5.2$ C/m^2; $e_{33}^{(1)} = 15.1$ C/m^2; $e_{15}^{(1)} = 12.7$ C/m^2; $\kappa_{11}^{(1)} = 730\varepsilon_0$; $\kappa_{33}^{(1)} = 635\varepsilon_0$; $\varepsilon_0 = 8.85 \cdot 10^{-12}$ F/m.

The geometric models of the composites with 3-0 connectivity were exported to binary format for the APDL ANSYS program. This program allows one to determine the effective moduli of the composite, based on the technique, described in [5].

Table 1 shows the effective moduli with a fixed percentage of inclusions (30%) with arbitrary random granule sizes and different number of finite elements in the representative volume of the composite (8, 16 or 32 elements along each side). The letters a, b and c indicate various starts of the granule generation program. Table 2 presents similar results for 60% of granules.

Table 1. Effective moduli with 30 % of inclusions.

	8a	8b	8c	16a	16b	16c	32a	32b	32c
Al_2O_3 (%)	29	30	30	30	30	30	30	30	30
$c_{11}^{\text{eff}}, 10^{10}$ N/m^2	21.3	21.9	21.7	20.5	21.1	20.9	20.4	20.3	20.4
$c_{12}^{\text{eff}}, 10^{10}$ N/m^2	9.1	9.3	9.2	9.1	9.1	9.2	9.2	9.2	9.2
$c_{13}^{\text{eff}}, 10^{10}$ N/m^2	8.7	8.9	8.9	8.8	8.7	8.7	8.7	8.7	8.7
$c_{33}^{\text{eff}}, 10^{10}$ N/m^2	19.7	20.9	20.5	20.0	19.8	19.8	19.4	19.5	19.3
$c_{44}^{\text{eff}}, 10^{10}$ N/m^2	5.8	6.4	6.1	5.8	5.6	5.8	5.4	5.5	5.4
e_{31}^{eff}, C/m^2	–3.8	–3.8	–3.9	–4.0	–3.9	–3.9	–3.9	–4.0	–4.0
e_{33}^{eff}, C/m^2	10.2	10.0	10.0	9.7	9.7	9.8	9.5	9.7	9.6
e_{15}^{eff}, C/m^2	8.9	8.4	8.9	8.5	8.9	8.7	8.8	8.6	8.8
$\kappa_{11}^{\text{eff}} / \varepsilon_0$	485	474	491	460	476	467	459	455	460
$\kappa_{33}^{\text{eff}} / \varepsilon_0$	425	423	421	405	405	407	393	400	397

Table 3 shows the effective moduli of the composite for various maximum granule sizes. The granule size is determined by the maximum and minimum number of finite elements. Calculations are performed for 30% and 60% inclusions. A representative volume includes 32 elements along each side (323 = 32,768 finite elements).

As can be seen from Tables 1 – 3, the representative volume sizes, as well as random choice of the granules and their sizes generally slightly affect the values of effective moduli, except for the moduli that have smaller values, compared to other moduli of the same types. Obviously, the greatest stability of results is achieved when increasing the number of elements in the representative volume. Thus, the smallest spread of data takes place for the representative volume with 32 elements along each side.

Table 2. Effective moduli with 60 % of inclusions.

	8a	8b	8c	16a	16b	16c	32a	32b	32c
Al_2O_3 (%)	59	59	64	62	60	62	61	61	61
$c_{11}^{\text{eff}}, 10^{10}$ N/m^2	31.9	31.5	32.9	31.4	29.9	31.1	30.3	30.3	30.3
$c_{12}^{\text{eff}}, 10^{10}$ N/m^2	11.3	10.8	11.2	11.1	11.0	11.2	11.1	11.1	11.1
$c_{13}^{\text{eff}}, 10^{10}$ N/m^2	10.5	10.9	11.0	10.6	10.6	10.6	10.6	10.6	10.5
$c_{33}^{\text{eff}}, 10^{10}$ N/m^2	30.0	31.2	32.4	30.9	30.2	30.7	30.3	30.3	30.3
$c_{44}^{\text{eff}}, 10^{10}$ N/m^2	10.1	10.3	10.8	10.2	9.9	10.2	9.8	9.8	9.7
e_{31}^{eff}, C/m^2	–1.5	–2.4	–2.0	–1.9	–2.2	–1.9	–2.1	–2.0	–2.0
e_{33}^{eff}, C/m^2	4.5	5.6	4.7	4.4	4.8	4.2	4.3	4.3	4.1
e_{15}^{eff}, C/m^2	5.2	4.8	4.4	4.0	4.3	3.9	4.1	4.0	4.2
$\kappa_{11}^{\text{eff}} / \varepsilon_0$	280	272	238	210	226	201	205	202	207
$\kappa_{33}^{\text{eff}} / \varepsilon_0$	185	243	203	184	202	175	180	178	171

Table 3. Effective moduli for different sizes of inclusions.

Size of granule (min-max)	1–300	1–200	1–100	1–50	1–300	1–200	1–100	1–50
Al_2O_3 (%)	30	30	29	30	61	59	61	57
$c_{11}^{\text{eff}}, 10^{10}$ N/m^2	20.3	20.2	20.3	20.5	30.2	30.1	30.5	29.3
$c_{12}^{\text{eff}}, 10^{10}$ N/m^2	9.2	9.2	9.2	9.2	11.1	11.0	11.1	10.9
$c_{13}^{\text{eff}}, 10^{10}$ N/m^2	8.7	8.8	8.7	8.7	10.5	10.0	10.6	10.3
$c_{33}^{\text{eff}}, 10^{10}$ N/m^2	19.4	19.2	19.3	19.5	30.3	29.8	30.3	29.1
$c_{44}^{\text{eff}}, 10^{10}$ N/m^2	5.5	5.5	5.4	5.5	9.8	9.6	9.8	9.4
e_{31}^{eff}, C/m^2	–4.0	–4.0	–4.0	–3.9	–2.0	–2.0	–2.0	–2.2
e_{33}^{eff}, C/m^2	9.6	9.7	9.6	9.7	4.3	4.3	4.3	4.8
e_{15}^{eff}, C/m^2	8.7	8.6	8.7	8.6	3.8	4.3	4.0	4.3
$\kappa_{11}^{\text{eff}} / \varepsilon_0$	456	455	460	458	191	214	201	222
$\kappa_{33}^{\text{eff}} / \varepsilon_0$	394	398	394	399	178	179	179	201

Figures 4 – 6 shows the dependence of the effective properties of the composite on the percentage content of the granule material in the volume at a fixed maximum number of finite elements in the representative volume (32,768 finite elements).

The dependencies shown in Figs. 4 – 6 completely correspond to the expected results. Since the inclusions are more rigid than the piezoceramic skeleton, the effective stiffness moduli increase with increasing the percentage of the inclusions. Moreover, since the moduli $c_{11}^{(2)} = c_{22}^{(2)} = c_{33}^{(2)}$ are the largest, then the effective moduli c_{11}^{eff} and c_{33}^{eff} grow faster than other moduli. In addition, since the inclusions are purely elastic and have small dielectric permittivities, both the effective piezomoduli and the effective dielectric permittivities decrease in magnitude with an increase in the inclusions fraction.

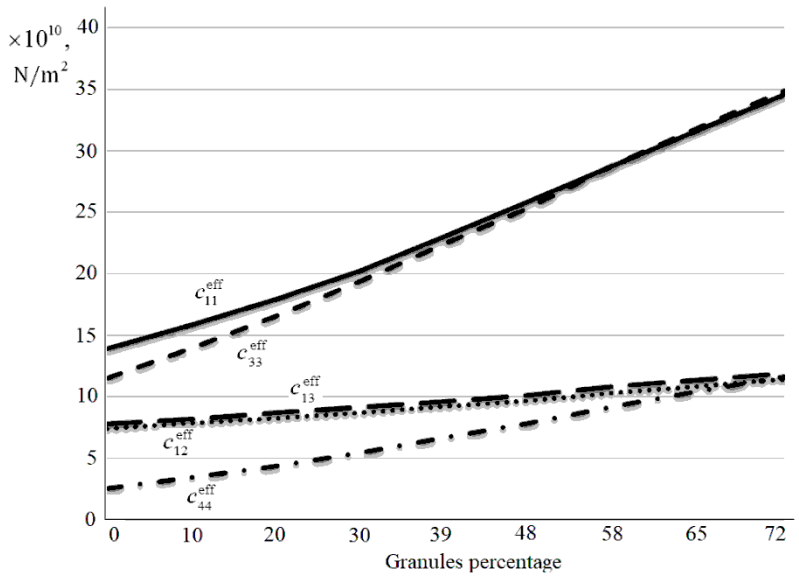

Fig. 4. Dependence of elastic stiffness moduli on the percentage of granules.

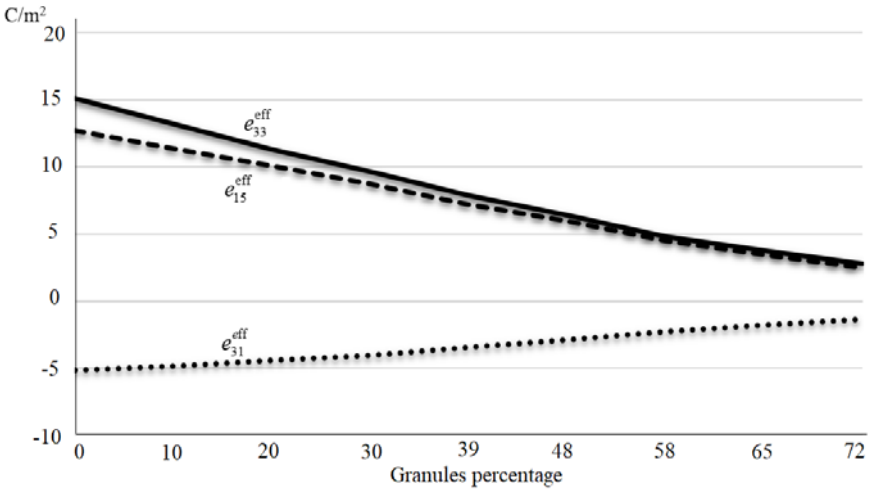

Fig. 5. Dependence of piezoelectric moduli on the percentage of granules.

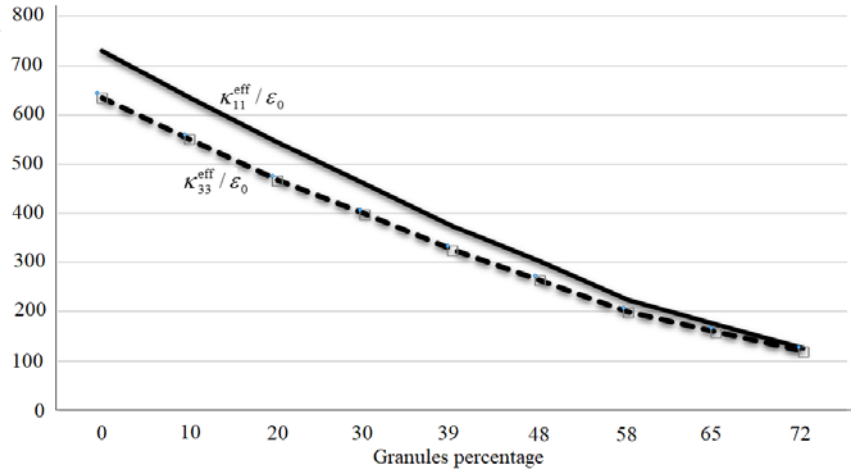

Fig. 6. Dependence of dielectric permittivity moduli on the percentage of granules.

We would like to note that the algorithm of the representative volume generation has the following interesting features. Numerical experiments showed that the result of the representative volume generation depend not only on the size of the cluster, but also on the range of the allowed granule sizes. Dimensions of granules are measured in the number of final elements. By default, the algorithm generates the granules with the sizes from 1 to 300 elements. By limiting the range of granule sizes, it is possible to obtain a model with approximately the same size of inclusions. However, in some cases the requirement on inclusion percentage can be violated. An experiment on generating the samples of materials with different fractions of the volume content of granules was carried out using the widest range of sizes 1 – 300 and several narrower ranges. The results of this experiment showed that for a significant range of sizes with a lower threshold the algorithm was able to generate models, corresponding to the input requirements. However, increasing the lower range limit narrows the scope of the algorithm applicability and leads to an increase in the relative deviation from the required percentage of the bulk content of the granule material.

5. Conclusions

The paper presents the homogenization methods for piezoelectric composites and the algorithm for generating a representative volume with 3-0 connectivity, implemented in the ACELAN-COMPOS package. The algorithm allows adjusting the percentage of granules in the composite, the size of the granules and the number of final elements in the representative volume. Numerical experiments were carried out to determine the range of applicability of the algorithm and to calculate the effective material properties of the composite depending on the input parameters of the algorithm.

Acknowledgement. *The work was supported by the Ministry of Education and Science of Russia, competitive part of state assignment, No. 9.1001.2017/PCh.*

References

[1] A.N. Rybyanets, A.A. Rybyanets // *IEEE Trans. Ultrason. Ferroelectr. Freq. Control* **58(9)** (2011) 1757.

[2] A. Rybyanets, A. Nasedkin, T. Domashenkina, A. Rybyanets, M. Lugovaya, In: *Proc. 2009 IEEE Ultrason. Symp., Roma, Italy, Sept. 20-23, 2009* (IEEE Publ., 2009), p. 1699.

[3] N.V. Kurbatova, D.K. Nadolin, A.V. Nasedkin, A.A. Nasedkina, P.A. Oganesyan, A.S. Skaliukh, A.N. Soloviev, In: *Advanced Structured Materials*, **59** (Springer, Singapore, 2017), 133.

[4] R.E. Newnham, D.P. Skinner, L.E. Cross // *Mater. Res. Bull*. **13(5)** (1978) 525.

[5] A.V. Nasedkin, M.S. Shevtsova, In: *Ferroelectrics and Superconductors: Properties and Applications*, ed. by I.A. Parinov (Nova Science Publishers, NY, 2011), p. 231.

[6] S.V. Bobrov, A.V. Nasedkin, A.N. Rybjanets, In: *Proc. VIII Int. Conf. on Computational Structures Technology*, ed.by B.H.V. Topping, G. Montero, R. Montenegro (Civil-Comp Press, Stirlingshire, UK, 2006), Paper 107.